Materials Science-Poland, Vol. 25, No. 4, 2007

Mechanism of charge generation and photovoltaic effects in lead phthalocyanine based Schottky barrier

G. D. SHARMA* , V. S. CHOUDHARY, Y. JANU, M. S. ROY

Molecular Electronics and Optoelectronics Devices Laboratory,
Department of Physics, J.N.V. University, Defence Laboratory, Jodhpur, India

Photovoltaic properties of lead phtalocyanine (PbPc) thin films sandwiched between indium tin oxide (ITO) and aluminum electrodes (ITO/PbPc/Al) have been investigated. The *J–V* characteristics of the device reveals that current flow across the device is limited by hole injection at Al/PbPc below 300 K, wherein Al is kept at higher bias. Junction parameters such as built-in potential (V_{bi}), carrier concentration (N_a), the width of depletion layer (W) were evaluated from the *C–V* measurements. The mechanism of transport of carriers in Al/PbPc/ITO has been investigated based on the detailed analysis of current–voltage characteristics at various temperatures in the dark. The PbPc form hole injection barriers with both Al and ITO electrodes which are 0.88 eV and 0.11 eV, respectively, indicating the formation of nearly Ohmic contact with ITO and the Schottky barrier with Al. The photovoltaic parameters of the device have been estimated from the analysis of the current–voltage characteristics under illumination and discussed in detail. Electrically active defects were investigated by the space charge capacitance spectroscopy methods at various temperatures (from 250 K to 350 K) and frequencies (from 5 Hz to 1 MHz), respectively. The activation energy calculated from the capacitance spectroscopy at various temperatures is about 0.32 eV suggesting that the defects originate from the trapping centres at Al/PbPc interface.

Key words: *charge generation; photovoltaic effect; lead phthalocyanine; Schottky barrier*

1. Introduction

During the last couple of decades, much effort has been put into the development of solar cells based on organic electronic materials because of their low cost and easy fabrication [1–8]. In molecular materials, the relevant molecules can be easily prepared and their properties modified to meet the optical and electronics requirements. Among a variety of molecular materials, phthalocyanines (Pcs) are well known stable materials with versatile functions [9–11]. Phthalocyanine molecule contains four iso-

*Corresponding author, e-mail: sharmagd_in@yahoo.com; on sabbatical leave from JNV University, Jodhpur (Raj), present address : MIT, Mandsaur (MP), India.

indole units (pyrrole ring conjugated with benzene ring). A large family of Pcs can be chemically modified by attaching various peripheral groups to outer ring of isoindoles. The difference in the molecular structure leads to the difference in their photophysical properties. Pcs absorb light in various spectral regions between 500 nm and 720 nm. Photovoltaic devices made from organic pigments reach power conversion efficiency of a few percent [10, 11] that is much lower than those of their inorganic counterparts, demanding further research for more efficient organic materials and their combinations. One of possible improvements for this type of photovoltaic devices is implementation of new materials, absorbing red or near infrared part of the solar spectrum, where maximum photon flux of the Sun light is located. Up till now CuPcs are among the promising donor materials for organic solar cells [12]. Lead phthalocyanine (PbPc) can also be used as a donor absorbing light in the range of 550–700 nm with absorption maximum about 680 nm and absorption edge around 740 nm. PbPc has received much attention as a promising material for gas sensor but it has not been explored in photovoltaic devices.

In the present work, we have characterized lead phthalocyanine (PbPc) in the form of a Schottky barrier device and investigated the mechanism of charge generation and photovoltaic response. PbPc is a p type organic semiconductor possessing high thermal stability and narrow optical band gap. We have studied the temperature dependence of current–voltage (J–V) characteristics of PbPc thin films sandwiched between indium tin oxide (ITO) and Al electrodes (Al/PbPc/ITO), with the aim to understand the charge generation mechanism and photovoltaic response in this device. The variation of concentration of injected charge carriers and their mobility with temperature, bias voltage carrier trap density arising due to the defects and impurities are very important information required for improving the device performance. The measurements of J–V characteristics at various temperatures and electric fields have been used as powerful tools for the above mentioned studies. We have shown that the measured current in ITO/PbPc/Al device is limited by hole injection at Al–PbPc contact when the device is reverse biased. The current becomes space charge limited at high voltages when tunnelling contributes significantly to charge injection.

2. Experimental

Thin films of PbPc were deposited on cleaned ITO coated glass substrates by spin coating technique employing ethanol containing DMSO as a solvent for PbPc. The thickness of the PbPc layer was controlled by the concentration of PbPc in solvent and rotation speed (about 2500 r.p.m.). The top electrode contact was made by evaporation of aluminum through an appropriate mask at a vacuum of 10^{-5} Torr. The resulting area of the device was about 1 cm^2. The optical absorption spectrum was recorded on 100 nm thin film of PbPc layer on a glass slide employing a Perkin Elmer double beam spectrophotometer. The cyclic voltammetry experiment was performed with

AutoLab potentiostat at room temperature in a conventional three electrode cell with ITO as the working electrode. For the current–voltage measurements, a Keithley electrometer with built in power supply was used. The capacitance spectroscopy and capacitance–voltage (*C–V*) measurements were recorded using an HP 4294 A impedance analyzer in parallel RC equivalent circuit mode, in the frequency range between 5 Hz and 10 MHz. The temperature of device was measured with a digital temperature controller and monitored by an indicator. The incident light was provided with a 100 W halogen lamp and the intensity of the light was measured by a lux meter. The photoaction spectra of the device were measured employing a monochromator with a halogen lamp as a source. The electrodes were illuminated through both sides of the electrodes and the resulting photocurrent was monitored with a Keithley electrometer.

3. Results and discussion

3.1. Current–voltage characteristics in dark

Current–voltage characteristics of the ITO/PbPc/Al device recorded at various temperatures ranging from 250 K to 350 K is shown in Fig. 1 in semi-log scale. The forward bias was obtained with positive and negative bias to ITO and Al electrodes, respectively. The asymmetrical nature of curves is attributed to the difference in work function of the electrodes, implying different barriers at each electrode/PbPc interface. As PbPc is a p type organic semiconductor, we assume that Al and ITO form Schottky barrier and nearly ohmic contact with PbPc, respectively, giving rise to asymmetrical nature of *J–V* characteristics, i.e. to the rectification effect.

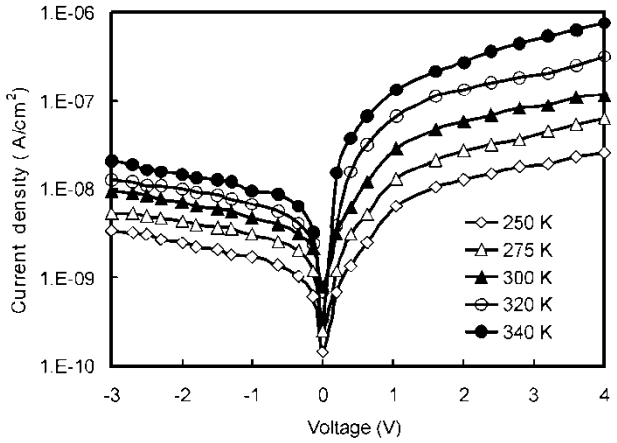

Fig. 1. Current–voltage characteristics of Al/PbPc/ITO device in dark at various temperatures when positive bias is applied to ITO

Figure 2a shows typical *J–V* characteristics of an ITO/PbPc/Al device in log–log scale at various temperatures when Al is negatively biased with respect to ITO. This situation corresponds to hole injection in the HOMO of PbPc through ITO and electron injection through Al into LUMO of PbPc. In each case, two distinct regions were observed in *J–V* characteristics of the device at temperatures below 300 K. At low voltages, the slopes of log*J* vs. log*V* plots are approximately equal to unity, while at higher voltages above a well defined transit voltage, the slopes are approximately between 2.0 and 2.5. These plots are typical of ohmic conduction at low voltages. It is well known that metal phthalocyanines (MPcs) are p type organic semiconductors, the conduction is via holes only, and the current may be simply expressed in the form [13]

$$J = p_0 q \mu \left(\frac{V}{d} \right)$$

where p_0 is the concentration of thermally generated holes, q is the electronic charge, μ is the hole mobility, V is the applied voltage and d is the thickness of the PbPc layer. At high voltage range, the power law dependence of $J(V)$ is indicative of space charge limited conductivity (SCLC) controlled by single dominant trapping.

The *J–V* characteristics of metal–organic semiconductor devices are controlled by two basic processes: injection of the charge carriers from electrodes into organic semiconductor and vice versa and transport of the charge carriers in the bulk of film. Steady state current is determined by the applied electric field, height of the injection barrier, i.e. difference between electrode work function and corresponding transport levels of the organic semiconductor and temperature. The current is either injection limited or bulk transport limited. For the injection of charge carriers into the organic semiconductor, the charge carriers must overcome a potential barrier at the electrode –organic semiconductor interface. In the case of small barrier or at high temperatures, a large number of charge carriers will have energies large enough to cross the interface barrier, hence thermionic emission takes place. But when temperature decreases or when the barrier height is large, a reduced number of charge carriers have energies larger than the potential barrier and therefore thermionic emission becomes insignificant. In this case injection occurs via quantum mechanical tunneling through the potential barrier.

The Al contact with organic semiconductor form a relatively high barrier at low temperatures and therefore thermally generated carriers are few and the injected charge density is small so that the overall behaviour becomes ohmic. As the voltage is increased, the number of injected carriers increases so that space charge accumulates limiting the current. The number of thermally generated carriers increases with temperature, therefore the current increases with temperature. The superlinear behaviour seen in the Fig. 2 suggests that the injected charge carrier overcomes the transport capabilities of PbPc, hence giving rise to the accumulation of positive charge near the Al hole injecting electrode and the bulk properties of the organic layer control the *J–V* characteristics.

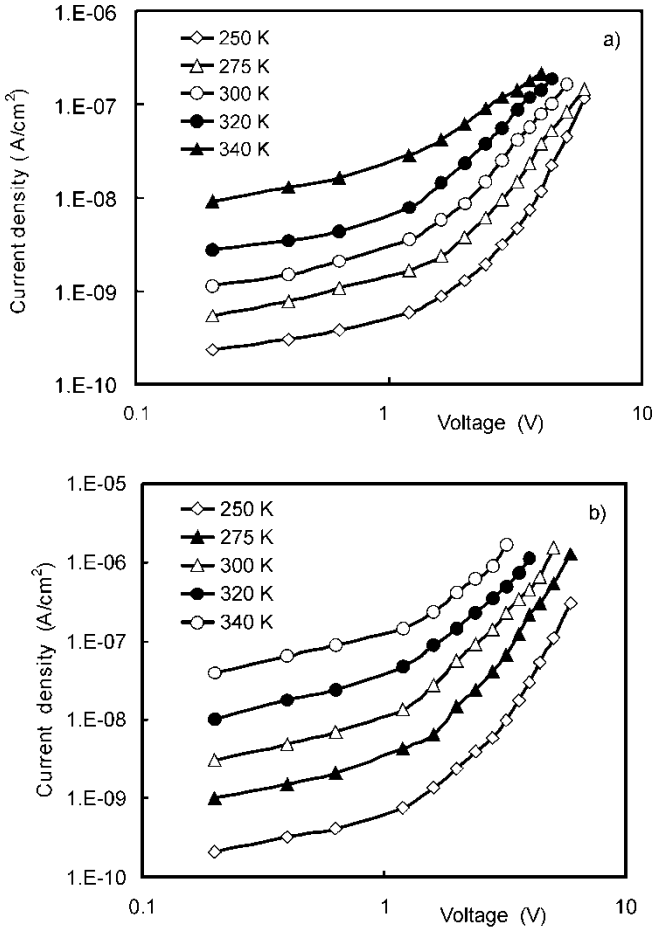

Fig. 2. Current–voltage characteristics in log–log scale for Al/PbPc/ITO device when Al (a) or ITO (b) are positively biased

The current–voltage characteristics shown in Fig. 2b have been measured with ITO as positively biased with respect to Al. This corresponds to the electron injection into the LUMO and hole injection into the HOMO of PbPc through Al and ITO, respectively. In this case the slope of *J–V* characteristics below 1.5 V is approximately two, which is an indication of SCLC behaviour. The injection of holes from ITO into HOMO of PbPc is more due to the low barrier for holes (as the ITO form nearly ohmic contact with PbPc) and injected carrier density becomes so large that the field due to the carriers themselves dominates over the applied field and becomes space charge limited. SCLC occurs when the transit time of any excess injected carrier is shorter than the bulk relaxation time. Under these conditions, the space charge limited current (TFSCLC) flows, as described by [14]:

$$J_{\mathrm{SCLC}} = \frac{9\varepsilon\mu V^2}{8d^3} \tag{2}$$

where μ is the effective mobility of charge carrier, ε – electric permittivity of PbPc, V is applied voltage and d is the thickness of the PbPc layer. This behaviour is characterized by a quadratic dependence of the current on voltage, i.e. the slope of J–V curve in the log–log scale is two. At higher temperatures, the slope of J–V curves is between 1 and 2. This indicates that the thermally generated carrier density exceeds that of the injected charges. The change in slope with applied voltages as seen in Fig. 2a, b are different due to the different hole injection barriers.

In the case when Al is positively biased, the slope of log$J$ vs. log$V$ curve is about unity, the region is considered as ohmic. Above the ohmic region, the J–V characteristics may be fitted to the Richardson–Schottky (RS) emission model. At higher fields, the metal work function for thermionic emission is reduced, thus lowering the Schottky barrier (image force lowering). The Schottky equation, taking into account image force lowering may be written as [15,16]

$$J = A^* T^2 \exp\left(-\frac{\varphi_b}{kT}\right)\exp\left[\frac{\left(\frac{q^3 V}{4\pi\varepsilon d}\right)^{1/2}}{kT}\right] \tag{3}$$

where V is applied voltage, positive for forward bias and negative for reverse bias. The equation can be rewritten as

$$\ln\frac{J}{T^2} = \ln A^* + \frac{-\varphi_b + \left(\frac{q^3 V}{4\pi\varepsilon d}\right)^{1/2}}{kT} \tag{4}$$

According to above equation, the plots of $\ln(J/T^2)$ vs. $1000/T$ are straight lines at a given bias voltage V. The effective barrier between the electrode and organic film may be calculated from the slope of the straight line as

$$\varphi_b = kS + \left(\frac{q^3 V}{4\pi\varepsilon d}\right)^{1/2} \tag{5}$$

where S is slope of the straight line. As seen from the Fig. 3, the plots of $\ln(J/T^2)$ vs. $1000/T$ at various voltages tend to be straight lines at higher temperatures. This is particularly clear in the case when ITO is positively biased, the straight line observed beyond room temperature (300 K) (Fig. 3a). When Al is positively biased (Fig. 3b), the linearity occurs at above 320 K. However, the domination of the thermionic emission observed at higher temperatures indicates that a higher hole injection barrier exists at Al/PbPc interface, since more thermal energy is required to overcome the potential barrier. Employing Eq. (5) and straight line fitting in Fig. 3 yield a hole injection

barrier equal to 0.11 eV and 0.88 eV for ITO/PbPc and Al/PbPc interfaces, respectively.

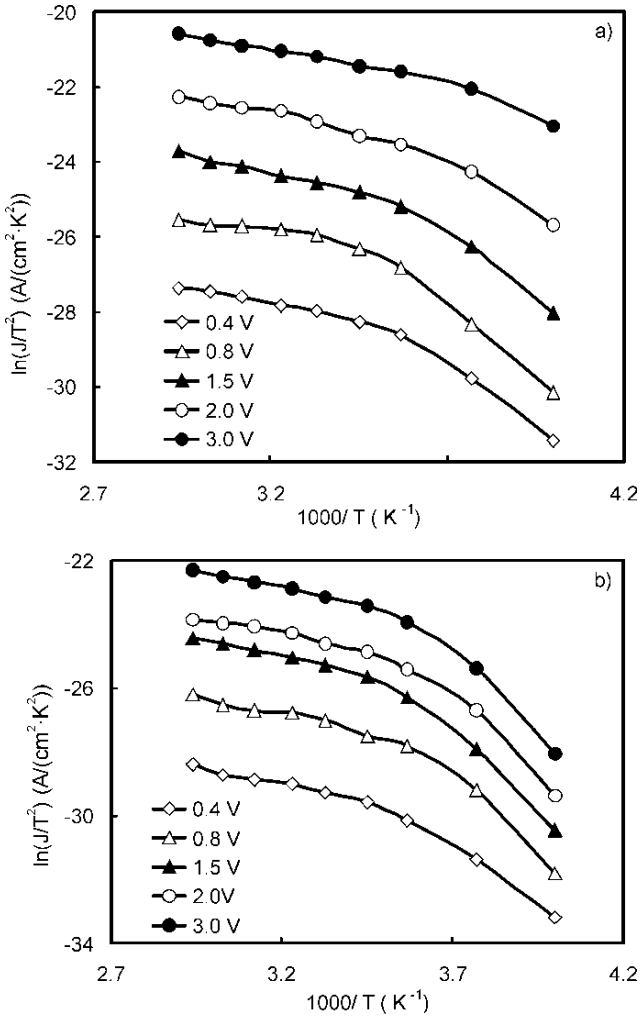

Fig. 3. $\ln(J/T^2)$ vs. $1000/T$ for Al/PbPc/ITO device when ITO (a) or Al (b) are biased positively

The electric field at which the transition from ohmic to SCLC takes place increases with temperature. In forward bias, the ITO/PbPc interface supplies a high amount of charges in PbPc bulk and the current is space charge limited in the whole voltage and temperature range, suggesting the formation of ohmic contact for hole injection at the ITO/PbPc interface.

The forward current density as a function of applied voltage at various temperatures shows non ideal junction characteristics (Fig. 1) and can be given by

$$J = J_{s1}[\exp(qV/nkT - 1] + J_{s2}[\exp(qV/2nkT) - 1] + \frac{J - JR_s}{R_{sh}} \tag{6}$$

where J_s is the reverse saturation current density, q is the electronic charge, V is the applied voltage, k is the Boltzmann constant, T is the temperature and n is the ideality factor of the diode. The subscripts 1 and 2 indicate that two possible contributions to the current could be present.

In a low forward voltage region ($0 < V < 0.6$ V) (as shown in Fig. 2b), the current density was suggested to be limited by the thermionic emission of holes from ITO over the ITO–PbPc barrier. According to the theory of thermionic emission mechanism, the forward bias current can be given by [17, 18]:

$$J = J_s[\exp(qN/nkT - 1] \tag{7}$$

The saturation current density J_s is given by

$$J_s = AT^2 \exp(-q\varphi_b/kT) \tag{8}$$

where A^* is the Richardson constant and ϕ_b is the barrier height. The values of n and J_s at room temperature were estimated to be 2.6 and 4.5×10^{-11} A/cm^2, respectively. The barrier height between ITO and PbPc layer being about 0.12 eV has been estimated in from Eq. (8), using Fig. 2b. This value is in good agreement with the value calculated from Eq. (5).

On the other hand, the current density as a function of applied voltage in the range 0.6 V$< V <$ 1.6 V, shows a power law dependence of the form $J \propto V^m$, where $m = 2$, indicating that the current density in the PbPc layer is an indication of SCLC. The current density in this region is given by Eq. (2). Note that the slope equal to two does not necessarily implies the absence of traps in the materials. Since the mobility of the charge carrier in organic semiconductor is so low that the extra injected charges cannot be swept to the collecting electrode at same time at which they are being injected.

As the voltage increases above 1.6 V, the current density in the PbPc layer is a space charge limited current (SCLC) dominated by a single trapping level. The current density in this region is given by [19, 20]:

$$J = \frac{9\varepsilon\mu_0\theta V^2}{8d^3} \tag{9}$$

where ε is the permittivity of PbPc, μ_0 is the mobility of a charge carrier taken as 7.8×10^{-4} cm^2/(V·s) at room temperature (calculated from the analysis of J–V characteristics at various temperatures), d is the thickness of the PbPc layer and θ is the trapping factor given by:

$$\theta = \frac{N_V}{N_t}\exp(-E_t/kT) \tag{10}$$

where N_V and N_t are the effective densities of states in the valence band and total trap concentration situated at energy level E_t above the valence band edge.

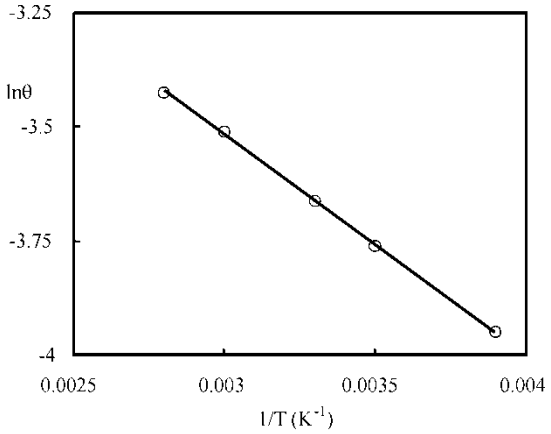

Fig. 4. Dependence of $\ln\theta$ on $1/T$ for Al/PbPc/ITO device

The values of θ corresponding to various temperatures can be estimated from the intercept of the straight line of $\log J$ vs. $\log V$ on current axis in the space charge region ($V > 1.6$ V). According to Eq. (10), the plot of $\ln\theta$ vs. $1//T$ is shown in Fig. 4. Assuming $N_v = 10^{27}$ m^{-3} [18], the analysis of Fig. 4 yields $N_t = 1.26\times10^{21}$ m^{-3} situated at 0.35 eV above the valance band edge. Similar values of the total trap concentration and trap energy levels for different metal phthalocyanines have been reported earlier [18–20].

3.2. Mobility calculations from *J–V* characteristics

It is observed that the *J–V* characteristics of the device, when positive voltage is applied to the ITO electrode, in the voltage range 0.6 V< V < 1.6 V, the current density in the entire temperature range varies in accordance with the relation for SCLC for trap filled organic materials described by Eq. (2). We have fitted our experimental results taking into account temperatures where *J–V* curves exhibited slope = 2 to Eq. (2), considering permittivity $\varepsilon = 3.4\times10^{-11}$ F/m and calculated the mobility under space charge limitation of current.

For low field region, the mobility is calculated at various temperatures using Eq. (2). The variation of the low field mobility with the temperature is shown in Fig. 5. It is found that the mobility is thermally activated in accordance with the relation

$$\mu = \mu_0 \exp[-\nabla/kT] \tag{11}$$

where μ_0 is the pre-exponential factor, ∇ is the thermal activation energy. The values of ∇ and μ_0 are found to be 0.31 eV and 5.78×10^{-4} cm^2/Vs, respectively. The plot of $\log\mu$ vs. 1000/T yields a straight line (Fig. 5), which indicates that the PbPc material is

inhomogeneous, i.e. the ordered regions are separated by amorphous regions. The activated behaviour of mobility is indication of inhomogeneity of the PbPc layer. A low value of the mobility activation energy represents the variation in the average energy of the adjacent hopping sites for polarons [21]. The charge transport occurs by hopping between adjacent sites through the disordered regions, which creates a potential barrier for the mobility of the carriers [22]. The mobility is therefore thermally activated and the value of thermal activation energy in PbPc film is lower than the in crystalline regions due to small sizes of amorphous regions.

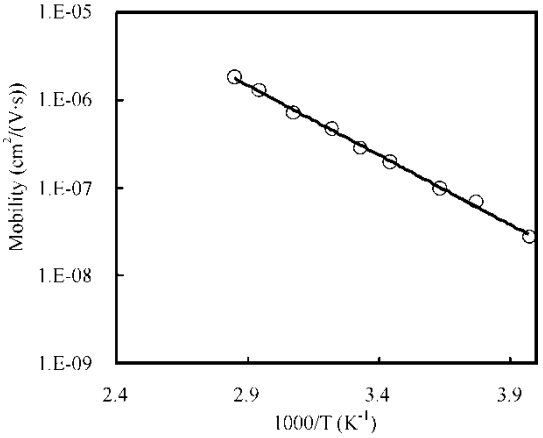

Fig. 5. Dependence of low field mobility on 1000/*T*

For bias voltages higher than 1.6 V, the current density does not follow Eq. (2). As the voltage increases, the barrier for the flow of holes from organic material into Al decreases and at sufficient high voltages, flat band condition is approached, i.e. the barrier at Al contact tends to zero. The current is now dominated by bulk of organic layer. The current in the bulk of the device is determined by the space charge created by injected carriers. Thus, as the voltage increases, the contact limited mechanism of current flow changes to the bulk limited mechanism.

At any temperature, the high bias field mobility can be fitted by [23]:

$$\mu(E) = \mu_0 \exp\left(\gamma\sqrt{E}\right) \tag{12}$$

where μ_0 is the low field mobility and the coefficient γ corresponds to the Poole Frenkel effect for disordered materials. This depends on the interaction between the charge carriers and randomly distributed dipoles in organic semiconductors [24]. The variation of $\mu(E)$ with E ($\log\mu$ vs. $E^{1/2}$) at room temperature is shown in Fig. 6. Similar variation of $\mu(E)$ is observed for other temperatures. The value of the slope of field dependence of mobility γ calculated from the slope of Fig. 6 is about 3.5×10^{-3} cm/V$^{1/2}$

and is found to decrease with the increase in temperature whereas the zero field mobility (the mobility extrapolated to zero field) is increasing with increasing temperature.

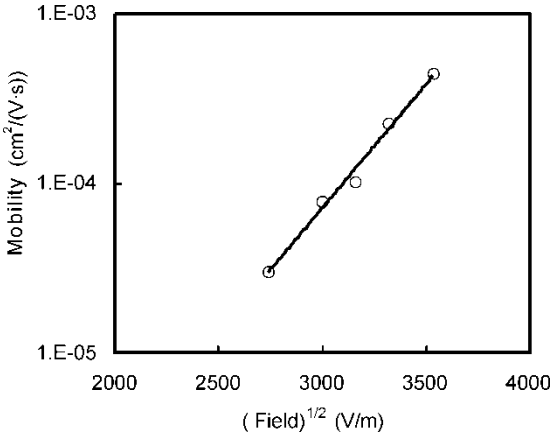

Fig. 6. Dependence of high field mobility on the square of electric field at room temperature

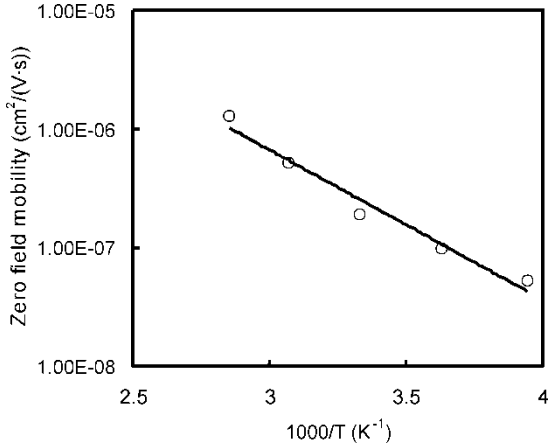

Fig. 7. Dependence of zero field mobility on 1000/*T*

Comparing Eqs. (11) and (12), the mobility variation with the field and temperature is given by

$$\mu(E,T) = [\mu_0 \exp(-\nabla/kT)]\exp(\beta\sqrt{E}/kT) \tag{13}$$

The expression in the bracket is field independent and μ_0 is the zero field mobility at any temperature *T*. The electric field helps the hopping carriers to overcome the potential barrier resulting in an increase of mobility with the increase in electric field *E*. The extrapolation of field dependences of the hole mobilities to zero field (Fig. 6) yields zero field mobilities at various temperatures and it is observed that it also shows

Arrhenius type temperature dependences (Fig. 7). From the slope and intercept of straight line ∇ and μ_0 are estimated to be 0.30 eV and 4.0×10^{-3}cm^2/(V·s), respectively. It is interesting to note that the value of ∇ is the same as calculated earlier. This relies upon the assumption that the charge transport is controlled by traps which are charged when empty, giving the Poole–Frenkel type mobility field dependences. It has been observed that the temperature dependence of the hole mobility in the PbPc shows an Arrhenius type behaviour and the energy of activation calculated has been found to show a negative field dependence.

3.3. Capacitance–voltage characteristics

In Figure 8, the capacitance spectrum at zero bias of the ITO/PbPc/Al device is shown at temperatures ranging between 250 K and 350 K and frequencies between 5 Hz and 1 MHz. One can notice the presence of steps due to the release of trapped charges from the trapping states. There is a shift of these steps to higher frequencies with increasing temperature, which indicates that the detrapping time constant of charge carriers is temperature dependent. Characteristic features of these states can be derived from the $C(f)$ spectra at certain critical frequencies ω_0, where an instantaneous decrease of the capacitance is observed.

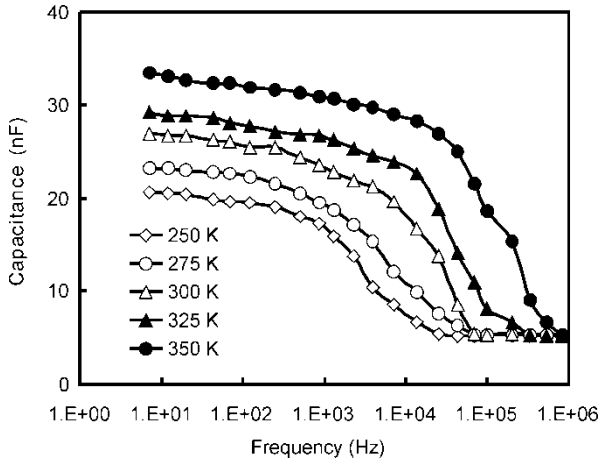

Fig. 8. Dependence of capacitance on frequency at various temperatures for Al/PbPc/ITO device

If a trapping state with the emission rate $\tau = 1/\omega_0$ is considered, the dependence of the capacitance on the frequency ω is given by [25]

$$C \propto \frac{\omega_0^2}{\omega + \omega_0^2} \tag{14}$$

The equation is a stepwise function, whereas the critical frequency ω_0 is the temperature-dependent parameter and can be described by the following expression

$$\omega_0 = \tau^{-1} = N_v \nu_{th} \sigma_h \exp(-E_a/kT) \tag{15}$$

where E_a is the activation energy, N_v is the effective density of states in valence band, ν_{th} is the thermal velocity of the charge carriers and σ_h is the capture cross section for holes. Assuming that $\nu_{\text{th}} \propto T^{1/2}$ and $N_v \propto T^{3/2}$, one may express Eq. (15) as

$$\omega_0 = \tau^{-1} = \xi_0 T^2 \sigma_h \exp(-E_a/kT) \tag{16}$$

where ξ_0 is the pre-exponential factor.

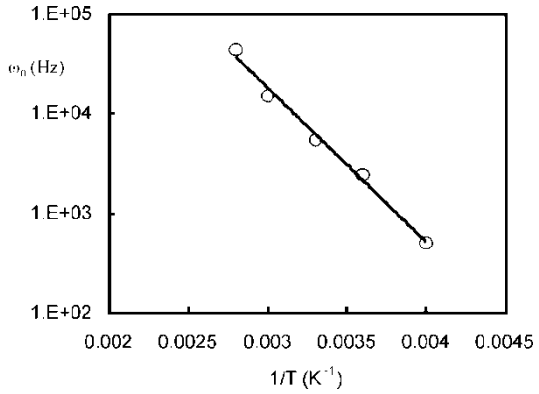

Fig. 9. Arrhenius plot of ω_0 for Al/PbPc/ITO device

Based on the model of Walter et. al. [26], from the minimum value of the capacitance derivative with respect to frequency at various temperatures, we have plotted ω_0 as a function of the reciprocal temperature T^{-1} (Fig. 9). We have calculated the activation energy form the slope of the Arrhenius plot and the temperature dependent pre-exponential factor $\nu_p = \xi_0 T^2 \sigma_h$ have been estimated from intercept on T^{-1} axis. The values of activation energy E_a and ν_p for PbPc are 0.32 eV and 8.0×10^8 s^{-1}, respectively, being in good agreement with the values reported for other metal phthalocyanines. The value of activation energy suggests that the defects originate from the trapping centres at the metal–PbPc interface. For the occurrence of these trapping centres, one would expect a weak bias sensitivity due to the hopping nature of the charge transport. At high electric field, the Coulomb barriers which separate adjacent hopping centres should be lowered or increased when the DC voltage is applied (Poole–Frenkel mechanism).

In the higher voltage region, we have also observed a change in the dominant conduction mechanism as shown in *J–V* characteristics in dark. The variation of log*J* with $V^{1/2}$ shows a linear relationship and is attributed to either the Poole–Frenkel (PF) or the Schottky effect [27]. Both mechanisms present a voltage variation described by:

$$J = J_0 \exp(AV^{1/2}) \tag{17}$$

where $A = \beta/kTd^{1/2}$, d is the film thickness and β is the field lowering coefficient which is twice higher in the PF effect as compared to the Schottky effect. β_{PF} is defined as

$$\beta_{PF} = \left(\frac{q^3}{\pi\varepsilon} \right)^{1/2} \tag{18}$$

where q is the electronic charge, and ε is the permittivity of the organic layer. From the J–$V^{1/2}$ plot we obtained the parameter A defined in Eq. (17) and consequently, the value of β. This value is approximately equal to β_{PF} calculated from Eq. (18) and is consistent with the values reported for other metal phthalocyanines for the Poole –Frenkel conduction is the Schottky junction [28, 29].

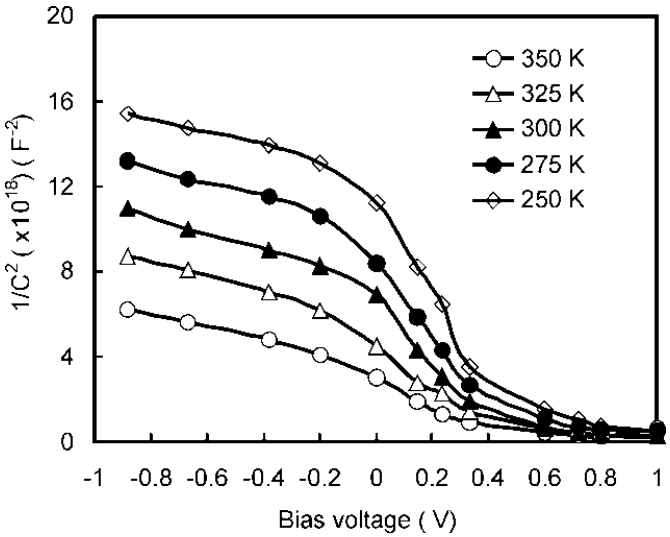

Fig. 10. Dependence of $1/C^2$ on bias voltage for Al/PbPc/ITO device at various temperatures

Figure 10 shows the $1/C^2$–V characteristics of the ITO/PbPc/Al device measured in dark at various temperatures at low frequency (40 Hz). The capacitance of the device can be expressed by two series: the junction capacitance C_j and the geometrical capacitance C_b referring to the bulk region of the PbPc; it can be expressed by

$$\frac{1}{C} = \frac{1}{C_j} + \frac{1}{C_b} \tag{19}$$

The dependence between C_j and the reverse bias for an abrupt junction can be described by [20, 30]:

$$\frac{1}{C_j} = \frac{2\left(V_{bi} - V_j - \dfrac{kT}{q}\right)}{q\varepsilon N_a A^2} \tag{20}$$

where V_{bi} is the built-in potential, N_a is the free carrier concentration, A is the effective surface area of the device and ε is the dielectric constant.

The carrier concentration can be experimentally estimated from [31]:

$$\frac{d\left(\dfrac{1}{C_j}\right)}{dV} = -\frac{2}{q\varepsilon N_a A^2} \tag{21}$$

where $d(1/C_j)/dV$ is the slope of the straight line and the intercept with the horizontal asymptote gives the built-in potential V_{bi} [32].

The asymptote represents the geometrical capacitance of the bulk region. The carrier concentration and built-in potential have been estimated (Table 1). The width of the depletion region W is related to the junction capacitance at V= 0:

$$W = \left(\frac{2\varepsilon V_{bi}}{qN_a}\right)^{1/2} \tag{22}$$

where ε is the permittivity of PbPc.

Table 1. Electrical parameters of Al/PbPc/ITO derived from capacitance–voltage characteristics at various temperatures

Parmeter	Temperature, T				
	250 K	275 K	300 K	325 K	350 K
V_{bi} (V)	0.65	0.63	0.61	0.59	0.58
ϕ_b (eV)	0.92	0.87	0.85	0.78	0.71
W (nm)	68	62	56	45	41
N_a (m^{-3})	2.3×10^{21}	6.7×10^{21}	2.3×10^{22}	5.6×10^{22}	8.9×10^{22}

The potential barrier ϕ_b between Al and PbPc has been calculated from the following expression:

$$\phi_b = V_{bi} + kT\ln\left(\frac{N_v}{N_a}\right) \tag{23}$$

where N_v is the density of states in valence band. The values of N_a, W and ϕ_b are presented in Table 1. The potential barrier at Al–PbPc in the device estimated from the C–V characteristics is almost equal to that calculated from the J–V characteristics.

3.4. Optical and photovoltaic properties

The energy gap was measured from the optical absorption curves, fitting data taken in the visible energy range. The energy gap $E_{g(\mathrm{opt})}$ is related to the absorbance α by Eq. (24), where $h\nu$ is the photon energy and A is a proportionality constant

$$\alpha h\nu = A\left(h\nu - E_{\mathrm{g(opt)}}\right)^{1/2} \tag{24}$$

The value of $E_{g(\mathrm{opt})}$ was determined by the extrapolation of the linear region to zero absorption [33], which is about 1.8 eV.

The energy levels for HOMO and LUMO of the PbPc were obtained by cyclic voltammetry with the method described by Bredas et al. [34]. The value of HOMO and LUMO levels for PbPc are 5.2 eV and 3.5 eV, respectively. These values lead us to electrochemical energy band gap for PbPc being about 1.7 eV, which is in a good agreement with those reported for other metal phthalocyanines [29, 35] from photo-emission spectroscopy and cyclic voltammetry measurements.

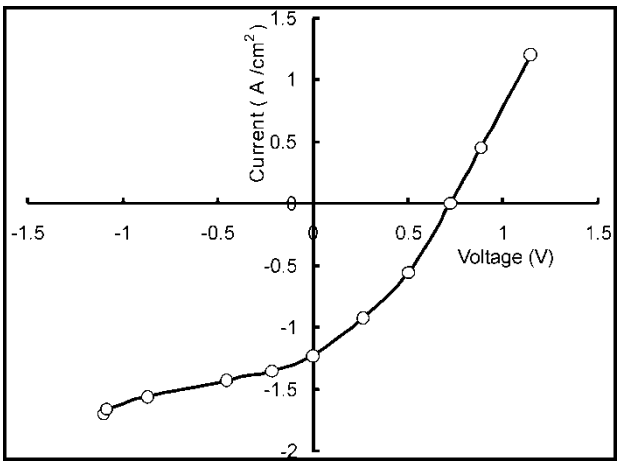

Fig. 11. *J–V* characteristics under illumination for Al/PbPc/ITO device at room temperature

The current–voltage characteristics of the Al/PbPc/ITO device under illumination of 5 mW/cm^2 is shown in Fig. 11. The values of photovoltaic parameters, i.e. short circuit current J_{sc}, open circuit voltage V_{oc}, fill factor FF and power conversion efficiency η) have been calculated from the following expression [36]:

$$FF = \frac{V_m J_m}{V_{oc} J_{sc}} \tag{25}$$

and

$$\eta = \frac{J_{sc} V_{oc} FF}{P_{in}} \tag{26}$$

J_m and V_m are the current and voltage maximum values, respectively and P_{in} is the intensity of incident light. The variation of V_{oc} with incident intensity P_{in} (corrected for absorption by ITO) are shown in Fig. 12. We have found the following results: The short circuit photocurrent J_{sc} increases as $(P_{in})^{0.6}$ between 0.01 and 5 mW/cm^2 and tends to saturate beyond this value. The fill factor decreases slightly up to 0.1 mW/cm^2 and then saturates.

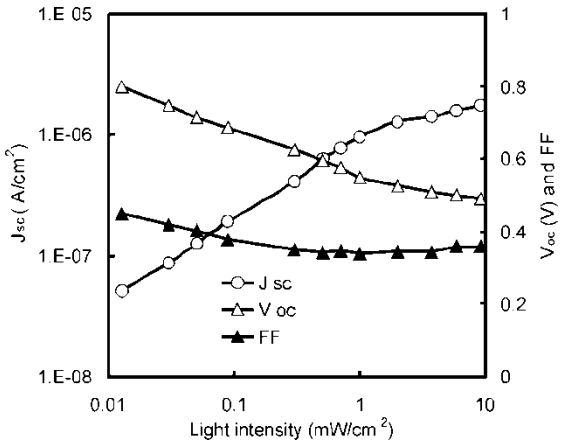

Fig. 12. Dependences of J_{sc}, V_{oc} and FF on the light intensity at room temperature

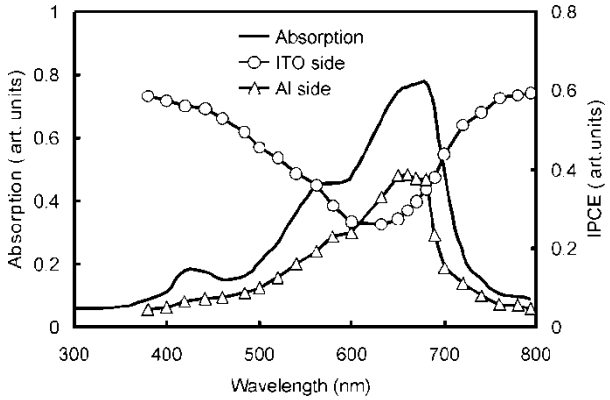

Fig. 13. Photoaction spectra for illumination of Al/PbPc/ITO device through ITO and Al electrodes along with absorption spectra of PbPc thin films

The consequence is a decrease in power conversion efficiency with P_{in}. The variation of short circuit photocurrent with light intensities below 1 mW/cm^2 indicates that photocur-

rent is limited by electron–hole bimolecular recombination leading to a decrease in over all power conversion efficiency. The values of short circuit photocurrent J_{sc}, open circuit voltage V_{oc}, fill factor FF and power conversion efficiency η are 1.23 μA/cm^2, 0.72 V, 0.43 and 0.077 %, respectively at the light intensity of 5 mW/cm^2.

Figure 13 shows the photoaction spectra of short circuit current for ITO/PbPc/Al Schottky barrier device illuminated through Al and ITO electrodes along with the spectrum of the PbPc layer. The absorption spectra of PbPc layer and photoaction spectra match fairly well when the device is illuminated through Al electrode. However, when the device is illuminated through ITO electrode, the photoaction spectra exhibit a minimum at the maximum of the absorption of PbPc layer. This behaviour is consistent with the Schottky junction located at the Al–PbPc interface which is responsible for the rectification behaviour observed in current–voltage characteristics in dark.

4. Conclusions

We have studied electrical and optical properties of the device based on PbPc sandwiched between Al and ITO. Based on the optical absorption spectra and cyclic voltammetry techniques, we have estimated optical and electrochemical band gaps of PbPc, being 1.8 eV and 1.7 eV, respectively. The current in this device is limited by hole injection at the Al/PbPc interface when the device is reverse biased and becomes space charge limited at high voltages, wherein tunneling contributes significantly to the charge injection. In the forward bias, the ITO/PbPc interface supplies high amount of charges in the PbPc bulk, and the current is space charge limited in the whole voltage range beyond 0.6 V, indicating the formation of an ohmic contact for hole injection at ITO/PbPc interface. From the detailed analysis of J–V characteristics, we have evaluated the potential barrier at Al/PbPc and ITO/PbPc, i.e. about 0.88 eV and 0.12 eV, respectively, which is in good agreement with the values calculated from the capacitance –voltage characteristics. The hole current is found to be space charge limited providing a direct measurement of mobility as a function of temperature and electric field. The hole mobility exhibits field dependence in accordance with the Poole–Frenkel effect.

Electroactive defects were also investigated by the space charge capacitance spectroscopy methods as a function of temperature and frequency in the range 250–350 K and 5 Hz–1 MHz, respectively. From the Arrhenius plots of critical frequency, we have concluded that the defects are thermally activated with the activation energy about 0.32 eV. The values of potential barrier and thickness of the depletion layer have also been estimated from the capacitance–voltage characteristics and found to be about 0.86 eV and 72 nm, respectively, and decreases with increasing temperature. The photoaction spectra of the device and optical absorption spectra of PbPc also lead to a conclusion regarding the formation of ohmic and Schottky barriers at ITO and Al contacts, respectively. The photovoltaic parameters of the device are: J_{sc} = 1.23 μA/cm^2, V_{oc} = 0.7 V, FF = 0.43 and η = 0.077 %.

Acknowledgement

We are grateful to the Department of Science and Technology, Govt of India, New Delhi for financial support through the project.

References

[1] WÖHRLE D., MEISSNER D., Adv. Mater., 3 (1991), 129.
[2] WHITLOCK J.B., PANAYOTATOS P., SHARMA G.D., COX M.D., SAUERS R.R., BIRD G.R., Opt. Eng., 32 (1993), 1921.
[3] ROSTALSKI J., MEISSNER M., Sol. Energ. Mater. Sol. Cells, 61 (2000), 78.
[4] SCHON J.H., KLOC CH., BUCHER E., BATTLOG B., Nature, 403 (2000), 408.
[5] WROBEL D., BOGUTA A., ION R.M., Int. J. Photoen., 2 (2000), 87.
[6] TANG C.W., Appl. Phys. Lett .,48 (1986), 183.
[7] PEUMANS P., YAKIMOV A., FORREST S.R., J. Appl. Phys., 93 (2003), 3693.
[8] *Organic photovoltaics*. *Concepts and Realisation*, Vol. 60, C.J. Brabec, V. Dyakonov, J. Parisi, N.S. Sariciftci (Eds.), Springer, Berlin, 2003.
[9] GREGG B.A., J. Phys. Chem B, 107 (2003), 4688.
[10] PEUMANS P., FORREST S.R., Appl. Phys. Lett., 79 (2001), 1261667.
[11] YAKIMOV A., FORREST S.R., Appl. Phys. Lett., 80 (2002), 1667.
[12] PEUMANS P., BULOVIC V., FORREST S.R., Appl. Phys. Lett., 76 (2000), 2650.
[13] LAMPERT M.A., MARK P., *Current Injection in Solids*, Academic Press, New York, 1970.
[14] ABKOWITZ M., FACCI J.S., REHM J., J. Appl. Phys., 83 (1998), 2670.
[15] BRAUN D., J. Polym. Sci. B, 41 (2003), 2622.
[16] KAO K.C., HWANG W., *Electrical Transport in Solids*, Pergamon Press, Oxford, 1981.
[17] ANTOHE S., TOMOZEIU N., GOGONEA S., Phys. Stat. Sol. (a), 125 (1991), 397.
[18] ANTHOPOULOS T.D., SHAFAI T.S., Phys. Stat. Sol. (a), 186 (2001), 89.
[19] SHARMA G.D., SANGODKAR S.G., ROY M.S., Mater. Sci. Eng. B, 41 (1996), 222.
[20] RIAD A.S., Physica B, 270 (1999), 148.
[21] RAKHMANOVA S.V., CONWELL E.M., Synth. Met., 116 (2001), 389.
[22] VISSENBERG M.C.J.M., BLOM P.W.M., Synth. Met., 102 (1999), 1053.
[23] CRONE B.K., DAVIDS P.S., CAMPBELL J.H., SMITH D.L., J. Appl. Phys.,84 (1998), 8333.
[24] DUNLAP D.H., PARRIS P.E., KENKRE V.M., Phys. Rev. Lett., 77 (1996), 542.
[25] HERBERHOLZ R., IGALSON M., SCHOCK H.W., J. Appl. Phys., 83 (1998), 318.
[26] WALTER T., HERBERHOLZ R., MULLER C., SCHOCK H.W., J. Appl. Phys., 80 (1996), 441.
[27] GOULD R.D., Coord. Chem. Rev., 156 (1996), 237.
[28] RASSAN A.K., GOULD R.D., Int. J. Electron., 69 (1990), 11.
[29] REIS F.T., MENCARAGLIA D., SAAD S.O., SEGUY I., OUKACHMIH M., JOLINAT P., DESTRUEL P., Synth. Met., 138 (2003), 33.
[30] ANTHOPOULOS T.D., SHAFAI T.S., Thin Solid Films, 441 (2003), 207.
[31] RIAD A.S., Thin Solid Films, 370 (2000), 253.
[32] ANTHOPOULOS T.D., SHAFAI T.S., J. Phys. Chem. Solids, 65 (2004), 1345.
[33] FUJITA S., NAKUZAWA T., ASANO M., FUJITA S., Jpn. J. Appl. Phys., 34 (2000), 5301.
[34] BRADES J.L., SILBEY R., BROUDREUX D.S., CHANCE R.R., J. Am. Chem. Soc., 105 (1983), 6555.
[35] ZHU L., TANG H., HARIMA Y., KUNUGI Y., YAMASHITA K., OHSHITA J., KUNAI A., Thin Solid Films, 396 (2001), 213.
[36] ASHOK S., PANDF K.P., Solar Cells, 14 (1985), 8.

Received 10 June 2007
Revised 25 July 2007